CVI
Journals.ASM.org

Establishment of a Swiss Webster Mouse Model of Pneumonic Plague To Meet Essential Data Elements under the Animal Rule

Patricia Fellows,[a] Winston Lin,[b] Carol Detrisac,[c] Shu-Chieh Hu,[b] Narayanan Rajendran,[b] Bruce Gingras,[b] Louis Holland,[b] Jessica Price,[a] Mark Bolanowski,[a]* and Robert V. House[a]

DynPort Vaccine Company LLC, A CSC Company, Frederick, Maryland, USA[a]; IIT Research Institute, Chicago, Illinois, USA[b]; and Charles River Laboratories, Pathology Associates, Chicago, Illinois, USA[c]

A recombinant vaccine (rF1V) is being developed for protection against pneumonic plague. This study was performed to address essential data elements to establish a well-characterized Swiss Webster mouse model for licensing the rF1V vaccine using the FDA's Animal Rule. These elements include the documentation of challenge material characteristics, aerosol exposure parameters, details of the onset and severity of clinical signs, pathophysiological response to disease, and relevance to human disease. Prior to animal exposures, an evaluation of the aerosol system was performed to determine and understand the variability of the aerosol exposure system. Standardized procedures for the preparation of *Yersinia pestis* challenge material also were developed. The 50% lethal dose (LD_{50}) was estimated to be 1,966 CFU using Probit analysis. Following the LD_{50} determination, pathology was evaluated by exposing mice to a target LD_{99} (42,890 CFU). Mice were euthanized at 12, 24, 36, 48, 60, and 72 h postexposure. At each time point, samples were collected for clinical pathology, detection of bacteria in blood and tissues, and pathology evaluations. A general increase in incidence and severity of microscopic findings was observed in the lung, lymph nodes, spleen, and liver from 36 to 72 h postchallenge. Similarly, the incidence and severity of pneumonia increased throughout the study; however, some mice died in the absence of pneumonia, suggesting that disease progression does not require the development of pneumonia. Disease pathology in the Swiss Webster mouse is similar to that observed in humans, demonstrating the utility of this pneumonic plague model that can be used by researchers investigating plague countermeasures.

Plague is caused by the Gram-negative bacterium *Yersinia pestis*. While natural outbreaks of disease occur in wildlife populations, humans are incidental victims in the life cycle of the bacterium in rodents. Human disease may also result from contact with blood or tissues of infected animals or exposure to aerosolized droplets containing bacteria (32, 37). Three forms of the disease exist and are believed to be dependent upon whether the bacteria enter the lymph nodes (bubonic), the bloodstream (septicemic), or the lungs (pneumonic).

Due to the potential person-to-person transmission of pneumonic plague, the Centers for Disease Control and Prevention (CDC) consider this disease to be a serious potential threat and have listed *Y. pestis* as a Category A threat, the highest-risk threat for potential bioterrorism agents (9). Aerosol dissemination represents the most plausible scenario for the use of *Y. pestis* as a biological weapon, with pneumonic plague being the most likely form of the disease that would occur following its use in a battlefield scenario or terrorist attack. In fact, the use of *Y. pestis* as a biological weapon is believed to have occurred as early as the mid-1330s on the Crimean coast (8, 25). In modern times, the use of *Y. pestis* by the Japanese Army during World War II as a potential biological weapon has been described (45), and the former Soviet Union is thought to have created highly lethal strains of *Y. pestis* in the 1970s and 1980s for a similar purpose (5).

Currently, no licensed plague vaccines are available for human use in the United States. The previously available U.S. Pharmacopeia vaccine was a killed, whole-cell vaccine that provided protection against bubonic plague but not pneumonic plague (3, 19, 24, 27). Significant local and systemic reactions also were reported following the administration of that vaccine (24, 27). Live attenuated vaccines have been used in several countries; however, due to considerable reactogenicity associated with these vaccines, they have not been licensed for use in the United States (17). Efforts to develop new plague vaccines have focused primarily on the proteins that play an important role in *Y. pestis* virulence, specifically the F1 capsular protein and V virulence proteins (3, 19, 49). The F1 protein forms a capsule-like structure on the surface of the bacterium that enables it to escape phagocytosis (46), and V antigen contributes to the type-three secretion system necessary for the *Yersinia* outer member proteins (Yops) to enter host cells (39). Antibodies against F1 (4) or V (23) protect mice against subcutaneous or aerosol challenge with *Y. pestis*. Furthermore, immunization with both F1 and V confers significantly higher levels of protection against both routes of challenge than immunization with either protein alone (19, 49). A recombinant plague vaccine (rF1V) composed of the F1 capsular protein and the V virulence protein fused into a single protein and formulated with alhydrogel is being developed by the U.S. Department of Defense to protect military personnel (ages 18 to 55) against battlefield exposures to aerosolized *Y. pestis* (29). Since the efficacy of the rF1V vaccine cannot be determined directly in humans and the incidence of pneumonic plague in the general population is low (50), the licensure of the rF1V vaccine will be sought based on meeting the requirements of the Animal Rule (13a).

Received 8 November 2011 **Returned for modification** 8 December 2011
Accepted 3 February 2012
Published ahead of print 15 February 2012
Address correspondence to Patricia Fellows, pfellows@csc.com.
* Present address: PharmAthene, Inc., Annapolis, Maryland, USA.

doi:10.1128/CVI.05591-11

There are several critical components in evaluating vaccine efficacy under the Animal Rule. Draft guidance provided by the FDA describes recommendations regarding route of exposure and challenge agent as well as design considerations in model development studies (10). Based on this guidance, animal models should be developed with both males and females using a route of exposure to the challenge agent that is the same as the anticipated human exposure route. Furthermore, the challenge agent used for animal studies should be identical to the etiological agent that causes human disease, and the material should be characterized to the fullest extent possible. Lastly, the reliable quantification and reproducibility of the challenge dosage should be documented.

This study was performed to address the essential data elements needed to establish a relevant animal model, as described in the FDA draft guidance document (10). The acceptance of the animal models for pneumonic plague and the subsequent evaluation of the rF1V vaccine involves the performance of well-controlled, well-documented studies that incorporate these requirements. A cynomolgus macaque model for pneumonic plague was recently developed (43), and the utility of the model in evaluating plague vaccine candidates was reported (13, 15, 26, 47). The development of a second animal model described here, the Swiss Webster mouse, facilitates meeting requirements of the Animal Rule.

MATERIALS AND METHODS

Animals. Equal numbers of male and female Swiss Webster (CFW) mice were obtained from Charles River Laboratories, Inc. (Portage, MI). Mice were approximately 9 weeks old at study initiation and ranged in weight from 22.6 to 35.5 g, with an average weight of 28.4 g. Animal housing consisted of plastic solid-bottom cages with hardwood chip bedding. Mice were provided food (certified rodent diet 5002; PMI Nutrition International, Inc., St. Louis, MO) and water *ad libitum*. Animal rooms were maintained at temperatures ranging from 22 to 24°C with alternating 12-h periods of light and dark and relative humidity ranging from 43 to 59%. Prior to exposure, all mice were acclimated during a 3-day period to the conditions experienced during the nose-only aerosol exposure to decrease stress on the day of exposure. Studies were conducted according to the principles set forth in the *Guide for the Care and Use of Laboratory Animals* (31) and adhered to all relevant federal guidelines and facility policies.

Characterization of *Y. pestis* CO92 banks. *Y. pestis* CO92 (*Orientialis* biovar), isolated from a fatal human case of pneumonic plague (16), was chosen as the challenge agent in the model development and subsequent rF1V vaccine efficacy studies. The strain is generally accepted as a standard challenge strain, and its use has been widely reported in the literature (2,3, 6, 19, 22, 35). Challenge material is considered a critical reagent, and using well-characterized material adds further control to the aerosol exposure system and confidence in subsequent data collected from animal studies. To ensure the quality and integrity of *Y. pestis* CO92, it was grown, characterized, and stored in a tiered banking system. The characterization testing of the banks was performed to ensure that preestablished technical specifications were met, including titer, purity, phenotype, growth curve, Gram stain, antibiotic susceptibility, glycerol fermentation, nitrate reduction, PCR, restriction fragment length polymorphism (RFLP), and multiple-locus variable-number tandem repeat analysis (MLVA). *In vivo* mouse pathogenicity was determined by conducting a subcutaneous 50% lethal dose (LD_{50}) determination study in equal numbers of male and female mice.

Challenge material. A standardized procedure was developed for the preparation of *Y. pestis* CO92 challenge material. Briefly, a frozen vial of the *Y. pestis* CO92 Working Cell Bank was thawed, and 500 μl was used to inoculate 100 ml of heart infusion broth plus 1.0% xylose (HIBx) in a 250-ml flask. The flask was incubated at 28 $\pm$ 2°C for approximately 18 h with shaking (200 $\pm$ 25 rpm). The optical density at 600 nm (OD_{600}) of the culture was adjusted to a final OD_{600} of 1 $\pm$ 0.1 with HIBx, which corresponded to a historical titer of 2×10^8 CFU/ml. Dilutions of the challenge material were prepared using phosphate-buffered saline to achieve the starting nebulizer concentrations required to achieve the target aerosol dosages. No additives, such as antifoam, were added to the challenge material preparation or to sample collection media in the all-glass impingers (AGI; Prizm Glass, Research Triangle Park, NC). The preparations were stored on ice until use.

Challenge material was also characterized for titer, phenotype, purity, and Gram stain each time it was prepared. Titer and phenotype were determined by plating dilutions of the challenge material in triplicate on tryptic soy agar and Congo red agar (CRA), respectively. Purity was evaluated by streaking for single-colony isolation on the following media: tryptic soy agar with 5% sheep blood, MacConkey agar, phenylethyl alcohol agar, and cefsulodin-Irgasan-novobiocin agar. A set of plates consisting of each medium type was incubated at three different temperatures (28 $\pm$ 2, 37 $\pm$ 2, and 23 $\pm$ 2°C) for a maximum of 14 days. Gram staining was performed using routine procedures.

Aerosol exposure system qualification. The aerosol route of exposure is the most relevant route of challenge for animal model development studies, as the rF1V vaccine is being developed to provide protection against pneumonic plague. Specifically, the nose-only route of exposure was chosen to ensure that all mice are exposed to an equivalent presented dosage of the challenge agent. Prior to conducting the LD_{50} and pathophysiology studies, the performance of the aerosol exposure system was characterized by evaluating spray factor, linearity of response, reproducibility, and particle size during 3 days of aerosol exposures in the absence of animals (sham exposures) with *Y. pestis* CO92. Spray factor is a unitless measurement and is defined as the ratio of the atmospheric concentration of the challenge material in the aerosol chamber to the starting concentration of challenge material in the nebulizer. It is a function of the aerosol generator, the biological agent, and the flow characteristics of the aerosol exposure system. Three nebulizer target concentrations (10^6, 10^7, and 10^8 CFU/ml) of *Y. pestis* CO92 were tested in triplicate during three separate days to determine run-to-run and day-to-day variability. These target nebulizer concentrations were chosen because they represented the range of target challenge dosages planned in subsequent mouse exposure studies. For each exposure, spray factor was calculated by dividing the chamber concentration by the starting nebulizer concentration. The spray factor provides an indication of the consistency of the aerosol system in delivering aerosolized *Y. pestis* at the target nebulizer concentrations. The particle size distribution of the aerosol was determined using a viable Anderson-type cascade impactor model TE-10-800 (Tisch Environmental, Cleveland, OH) operating at 28.3 liters per min (lpm). The mass median aerodynamic diameter (MMAD) was calculated based on the viable bacteria counts on CRA at each stage of the impactor process.

Aerosol exposure. The *Y. pestis* CO92 aerosols were generated using six Pari LC Plus nebulizers (Pari GmbH, Starnberg, Germany) connected to a custom-made glass mixing plenum. This configuration creates sufficient airflow in the exposure chamber to promote the mixing of the generated aerosol such that no additional dilution air is required. This prevents desiccation and the potential reduction of viability of the organism during the aerosolization process, thereby reducing the need to monitor humidity. Each Pari nebulizer operates at 20 lb/in^2 and produces airflow of approximately 4 to 5 lpm. Combining six Pari nebulizers has the net effect of producing approximately 25 to 30 lpm of airflow. Once the mixing of the aerosols occurs in the mixing plenum, the aerosols flow into the nose-only exposure chamber through a tube junction into the 64-port flow-past nose-only exposure chamber (Lab Products Inc., Seaford, DE). Temperature and airflow are monitored throughout the exposure. Incoming airflow is balanced with exhaust flow so that the overall pressure difference in the exposure chamber is close to zero. All exhaust air is filtered through dual HEPA filters. The aerosol chamber concentration is sampled using two AGIs (215 by 28 mm), each containing 10 ml of PBS,

TABLE 1 Pathophysiology study design

Group and treatment	No. of mice	Sample collection, h postchallenge					
		12	24	36	48	60	72
Aerosol exposure[a]							
1	20	X					
2	20		X				
3	20			X			
4	20				X		
5	20					X	
6	20						X
Baseline control[b]							
7	10	X					
Media controls[c]							
8	12	X					X

[a] Mice were challenged with a lethal dose of *Y. pestis* CO92 via nose-only exposure. At each time point, terminal blood samples were collected and pooled by sex for clinical chemistry and bacteremia determinations. Differential white blood cell counts and hematocrit were performed on individual samples. Gross necropsies, bacterial tissue burdens, and histopathology were completed at each time point.
[b] Untreated mice served as baseline controls for clinical chemistry and hematology.
[c] Aerosol exposure of control material consisting of fresh, sterile growth medium used to propagate *Y. pestis* CO92. Six mice (three males and three females) were euthanized at 12 and 72 h and served as pathology controls.

serially connected to a port in the exposure chamber. The primary AGI contained 2-mm beads to enhance collection efficiency by increasing surface area. AGI flow rate was controlled by a critical orifice at 1 ± 0.1 lpm. Unanesthetized mice were restrained in nose-only tubes and placed into the exposure tower such that only the mouse nose was exposed to the aerosol. Mice were exposed to the *Y. pestis* aerosol for 10 min to achieve the targeted aerosol dosage. The exposure chamber was sampled by the AGI for approximately 9 min. The purging of the aerosol system with clean air occurred for at least 5 min following aerosol exposure. Samples from the nebulizer and the AGIs were plated in quintuplicate on CRA to confirm the concentration of the starting material and to determine the concentration of the aerosol in each exposure. Respiratory minute volumes (RMV) were estimated for each mouse using Guyton's formula (18). Presented dosages were calculated based on RMV, exposure time, and aerosol concentration, as determined by AGI samples. The MMAD of the bacteria were determined for each aerosol exposure.

Aerosol LD_{50} determination. A total of 50 Swiss Webster mice (five males and five females per group) were challenged via the nose-only route of aerosol exposure. Targeted inhaled challenge dosages ranging from 2×10^2 to 2×10^5 CFU of *Y. pestis* CO92 were selected to confirm the LD_{50}. These dosages were selected based on data collected in a pilot study designed to evaluate the lethality of the *Y. pestis* CO92 Working Cell Bank (unpublished results). Mice were observed twice daily for clinical signs of disease and mortality for 14 days postchallenge.

Pathophysiology of disease. A total of 142 Swiss Webster mice (71 males and 71 females) were used to evaluate the pathophysiology of pneumonic plague. The study design is provided in Table 1. Mice in groups 1 through 6 were exposed by the nose-only route to an inhaled target dosage of 1 LD_{99} (4.3×10^4 CFU) of *Y. pestis* CO92 during multiple exposure runs on the same day. At 12, 24, 36, 48, 60, and 72 h postchallenge, samples were collected from mice in groups 1 to 6. Mice in group 7 were untreated and served as baseline controls for clinical chemistry and hematology. Mice in group 8 were exposed to aerosols of the fresh growth medium used to propagate the challenge material and were euthanized at 12 or 72 h postchallenge. These mice served as the controls for pathology evaluations.

Blood collection. Terminal blood samples were collected from each animal in groups 1 through 6 in the pathophysiology study (after isoflurane anesthesia) via retro-orbital sinus puncture for clinical chemistry, hematology, and bacteriological culture at 12, 24, 36, 48, 60, and 72 h postchallenge. Terminal samples were collected from the untreated controls (group 7) at 12 h and served as the baseline controls for clinical chemistry and hematology. Serum samples for clinical chemistry evaluations were pooled by collection time point and sex. They were analyzed using a Synchron LX20 Clinical Systems analyzer (Beckman Coulter, CA). Individual mouse samples were used to determine hematocrit and manual differential white blood cell counts. Paired capillary tubes from each individual mouse were spun for 5 min in a hematocrit centrifuge (BD-Clay Adams, NJ), and values were read with a Critocaps microhematocrit capillary tube reader. The two values were averaged and recorded as the percentage of packed red blood cells (RBC). Blood smears were stained using Wright-Giemsa staining methods with an automated staining system (Midas II Stainer; EM Science, Gibbstown, NJ), and manual differential counts of cells were performed. The remaining blood at each time point was pooled by sex for a qualitative assessment of bacteremia by plating 100 μl of the pooled blood sample onto CRA.

Necropsy and histopathology. All mice, with the exception of those in group 7, were subjected to necropsy. Tissues selected for microscopic evaluation were based upon a review of historical data (1) and included lung (with mainstem bronchi), trachea, lymph nodes (mandibular, axillary, inguinal, bronchial, and mediastinal), kidneys, spleen, and liver. Prior to tissue preservation in formalin, using a sterile technique, samples of the spleen, liver, kidney, and lung were collected for qualitative evaluation to determine the incidence of bacteria in each tissue. A sample of tissue from each organ was collected and placed into a tube containing 0.5 ml of 1% peptone. The tissue was homogenized using a disposable pestle (USA Scientific, Ocala, FL), and 100 μl was spread plated onto CRA. The plates were incubated for approximately 2 days at 28°C. Formalin-fixed tissues were routinely processed and paraffin embedded, and sections were stained with hematoxylin and eosin. Microscopic findings were graded semiquantitatively according to the following scale, with the associated numerical score used to calculate average severity grades for each lesion by group and sex. Lesions were graded on a scale of 1 to 4. Minimal (grade 1) represented the least detectable lesion; mild (grade 2) represented an easily discernible lesion unlikely to have biological relevance; moderate (grade 3) represented a change affecting a large area of represented tissues with the potential to be of some relevance; and marked (grade 4) represented a lesion that approached maximum relevance.

Statistical analysis. Probit analysis (Minitab, State College, PA) was used to estimate the LD_{50} and LD_{99} values. *t* test analysis (Microsoft Excel) was used to compare differential white blood cell count data for significance compared to the baseline controls.

RESULTS

Cell bank characterization. *Y. pestis* CO92 cell bank characterizations were previously performed (unpublished data). Briefly, results indicated that the banks are pure, Gram-negative cultures, with titers of $\geq 10^6$ CFU that exhibited 100% pigmented colonies when plated on CRA. Time course studies showed that cell growth exhibited characteristic lag, logarithmic, and stationary growth phases. Additional testing indicated that the banks demonstrated a positive result for nitrate reduction, a negative result for glycerol fermentation, and susceptibility to streptomycin, ciprofloxacin, tetracycline, gentamicin, and doxycycline. Genetic testing confirmed the presence of three plasmids (pCD1 [pYV], pMT1 [pFra], and pPCP1 [pPst]), identified banding patterns via RFLP, and determined that MLVA resulted in amplified loci differing by no more than five base pairs from predicted sizes. Finally, the LD_{50} of banked material was determined to be 1.5 CFU when administered by the subcutaneous route of injection.

Challenge material. Characterizations of the challenge material demonstrated that overnight cultures were Gram-negative,

TABLE 2 Summary of challenge data

Group	No. of mice	Target challenge dose (CFU)	Presented challenge dose (CFU)	% survival	Mean time to death (range), in days	SD
1	10	2×10^2	2.3×10^2	90	6.0	NA[a]
2	10	2×10^3	4.4×10^3	40	3.8 (3–5)	0.98
3	10	2×10^4	2.5×10^4	0	4.8 (3–7)	1.72
4	10	2×10^5	7.9×10^4	0	3.8 (3–6)	1.03
5	10	2×10^6	6.9×10^5	0	3.1 (3–4)	0.32

[a] NA, one mouse died on day 6.

pure cultures of *Y. pestis* with 100% pigmented colonies on CRA and had average concentrations of 3.9×10^8 and 2.2×10^8 CFU/ml for the LD_{50} and pathophysiology studies, respectively.

Characterization of the aerosol exposure system. The spray factor for each nebulizer concentration ranged from 1.3×10^{-5} for the highest nebulizer concentration (10^8 CFU/ml) to 1.1×10^{-5} for the lowest nebulizer concentration (10^6 CFU/ml), indicating that the efficiency of the aerosol exposure system was similar at the nebulizer concentrations tested. The run-to-run and day-to-day variability for each of the nebulizer concentrations was <3-fold, with one exception. On the second day of exposures, the run-to-run variability observed in the aerosol chamber concentrations with the 10^7 CFU/ml nebulizer concentration was 6.8-fold. The MMAD of the particles across all aerosol exposures ranged from 1.23 to 1.5 μm, which was in the respirable range (21).

Lethality. The target aerosol concentrations in the LD_{50} study ranged from 2×10^2 to 2×10^6 CFU/mouse, with presented dosages ranging from 2.3×10^2 to 6.9×10^5 CFU/mouse (Table 2). All mice in the 3 highest challenge dosage groups succumbed to disease following challenge, while 9 of 10 and 4 of 10 mice survived in the 2 lowest challenge dosage groups, respectively. Adverse clinical signs observed in the mice postchallenge included hunched posture, rough coat, and lethargy. While the onset of clinical signs was not associated with challenge dosage, the frequency of clinical signs was dosage related. Mean time to death (MTTD) generally trended lower with increasing challenge dosages. Using Probit analysis, the LD_{50} and LD_{99} were calculated to be 1,966 and 42,890 CFU, respectively (Table 3). The LD_{50} was similar to that previously determined (2,310 CFU; unpublished data) and falls within the infective dose range for a human, which is estimated to range from 5×10^2 to 1.5×10^4 organisms (40). The estimation of the LD_{99} was important in selecting the aerosol exposure level for the subsequent pathophysiology study and planned vaccine efficacy studies to ensure lethality in naïve animals.

Pathophysiology of disease. (i) Mortality and clinical observations. Presented dosages across the aerosol exposures ranged from 3.6×10^4 to 5.5×10^4 CFU/mouse. Adverse clinical signs observed in the mice postchallenge included hunched posture and rough coat. Lethargy was not observed in these mice. A separate group of mice challenged with *Y. pestis* CO92 served to ensure the lethality of the challenge dosage and were observed for 14 days postchallenge. All mice in this group died with an MTTD of 2.8 days (standard deviations [SD], 0.26; range, 2.5 to 3 days).

(ii) Clinical chemistry. The majority of the assays performed on pooled serum samples did not show remarkable trending. Two enzymes reflecting liver function, alanine aminotransferase (ALT) and aspartate aminotransferase (AST), demonstrated increases from baseline values at 48 and 72 h postchallenge (Fig. 1A and B). While levels of AST increased at these later time points, they were within the normal range (41). A third liver function enzyme, alkaline phosphatase (ALP), trended downward compared to baseline levels (Fig. 1C); however, values in the males were above the normal range at baseline. Lactate dehydrogenase (LDH), an indicator of primary muscle and hepatic damage, trended upward with a 3-fold increase from the baseline observed at the 72-h time point (Fig. 1D). The statistical significance of this trend could not be determined, since individual samples were not evaluated. Given the concurrent microscopic findings (discussed further below) in multiple tissues, these results appear to be relevant in the progression of disease following aerosol challenge with *Y. pestis* CO92 in mice.

TABLE 3 Estimates of inhaled LD_{50} and LD_{99} values with lower and upper 95% confidence intervals

LD	Dose (CFU/mouse)	95% confidence interval	
		Lower	Upper
50	1,966	672	4,366
99	42,890	14,183	802,597

(iii) Hematology. No differences in the individual hematocrit values during the 72-h collection period were observed. The average hematocrit value for all samples was 42.6% ± 3.1%. Differential white blood cell counts yielded a statistically significant ($P \leq 0.05$) increase in neutrophil percentages coupled with a concurrent statistically significant ($P \leq 0.05$) decrease in lymphocytes beginning at 36 h compared to baseline values. These significant differences were also observed at the 48-, 60-, and 72-h time points (Fig. 2). Differences in cell counts between male and female mice were observed only at the 72-h time point. While overall neutrophil counts were increased and lymphocyte counts decreased at this time point, female mice exhibited a significantly lower ($P \leq 0.05$) neutrophil count and a significantly higher ($P \leq 0.05$) lymphocyte count compared to male mice. Changes (morphological or percentage) were not observed in any other cell types counted.

(iv) Bacteria in blood and tissues. Qualitative assessments of bacteria in blood (pooled samples by group) and tissues were made at each sample collection time point. Bacteremia was detected at 24 h postchallenge in samples collected from females, whereas bacteremia was not detected until 36 h postchallenge in males. Bacteremia was detected in both males and females at all subsequent time points. The presence of bacteria in the lung, liver, kidney, and spleen was also assessed at each sample collection time point. The presence of bacteria was evident in lungs, as expected, for all animals starting at the 12-h time point, while bacteria in the liver, kidneys, or spleen were not detected until 24 h postchallenge. The numbers of mice with tissues testing positive for *Y. pestis* began increasing 24 h postchallenge and continued to increase throughout the collection time points (Table 4). The microscopic observations of bacteria in the lung and mandibular lymph node were noted 36 h postchallenge. By 48 h postchallenge, the number of tissues with microscopic observations of bacteria increased and generally continued to increase throughout the collection time points. While bacteria were isolated from the kidney using microbiological culture methods, they were not observed microscopically.

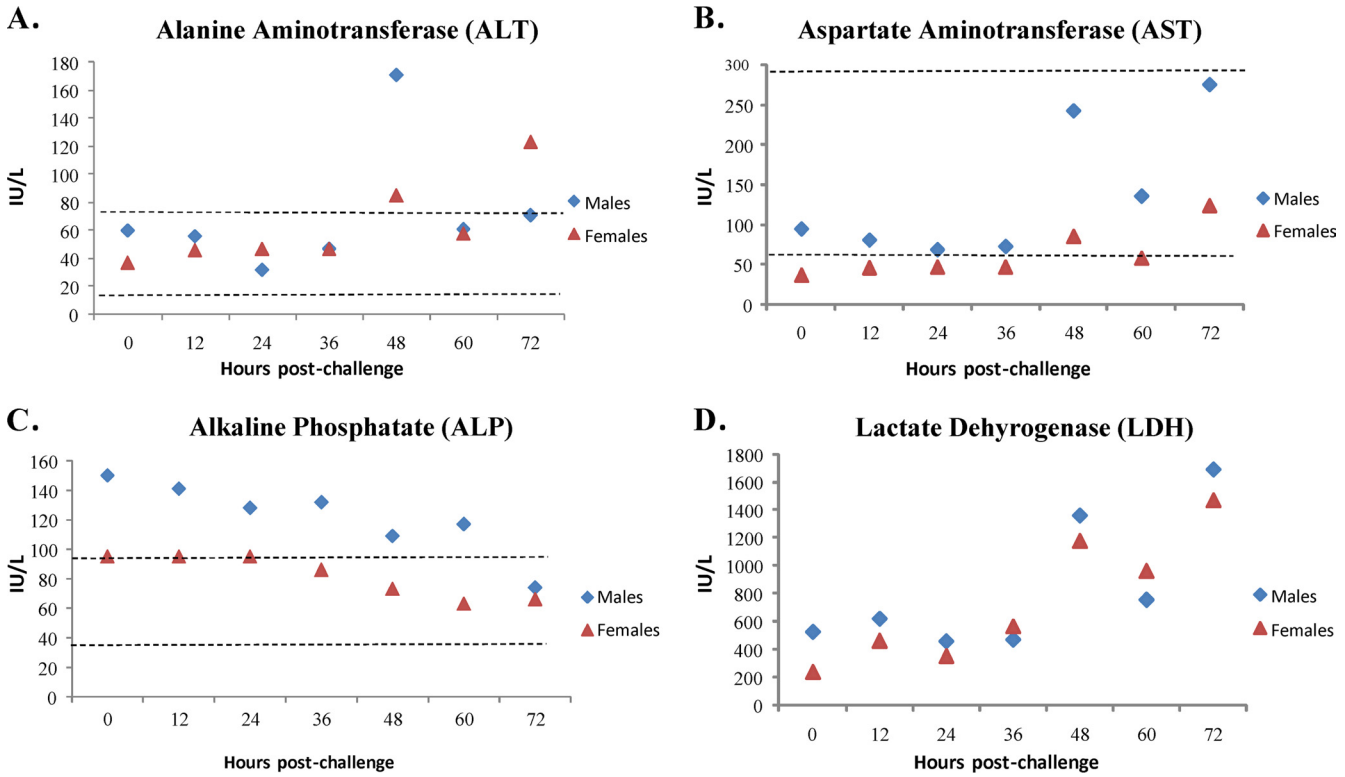

FIG 1 Data presented are results of clinical chemistry evaluations performed on serum samples pooled ($n = 10$) by sex at each collection time point along with the normal ranges (dotted lines), when available (41). Time zero represents baseline values determined from mice in group 7 and are shown in Table 1. (A) Alanine aminotransferase; (B) aspartate aminotransferase; (C) alkaline phosphate; and (D) lactate dehydrogenase. Diamonds, males; triangles, females.

(v) Necropsy and histopathology. The majority of the mice in the study were exposed to *Y. pestis* and euthanized at scheduled time points (every 12 h) postexposure. The prosectors and the pathologist were aware of the scheduled sample collections and therefore were not blinded. Necropsies were performed on 20 mice at each sample collection time point postchallenge.

At 12 and 24 h postchallenge, no gross lesions were present in any tissues examined that were considered plague related. By 36 h, enlarged mandibular lymph nodes and spleens were observed in both male and female mice. The incidence was 45% for the mandibular lymph node and 24% for the spleen. Over time the incidence of enlarged lymph nodes varied from 20 to 55% with no direct time relationship until 72 h postchallenge (55%). Similarly, the incidence of enlarged spleens varied between 20 and 25% until the 72-h time point, when the incidence was 40%. Gross lesions were not identified in the kidney or liver at any time point.

Mice challenged with *Y. pestis* CO92 and euthanized 12 h postchallenge did not have microscopic lesions in the lungs, lymph nodes, liver, spleen, or kidneys considered to be associated with *Y. pestis* infection. Pneumonia was defined as the presence of a minimal to moderate inflammatory cell infiltrate. At 24 h postchallenge, the only mouse with microscopic lesions had minimal focal mixed-cell infiltrate (neutrophils, macrophages, and lympho-

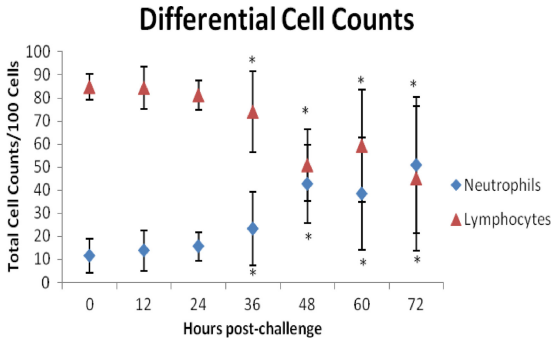

FIG 2 Data presented are averages from individual results ($n = 10$, both sexes) of manual differential counts of neutrophils and lymphocytes. Time zero represents baseline values determined from mice in group 7 and are shown in Table 1. Error bars represent standard deviations. Diamonds, neutrophils; triangles, lymphocytes. An asterisk indicates a statistically significant ($P < 0.05$) increase in neutrophils and a concurrent statistically significant ($P < 0.05$) decrease in lymphocytes from baseline values.

TABLE 4 Qualitative assessments of bacteria in tissues

Tissue	No. (%) of animals positive for *Y. pestis* in each tissue at each collection point, h postchallenge					
	12	24	36	48	60	72
Lung	20 (100)	18 (90)	19[a] (100)	20 (100)	20 (100)	20 (100)
Liver	0 (0)	8 (40)	13 (65)	17 (85)	18 (90)	17 (85)
Kidney	0 (0)	16 (80)	11 (55)	16 (80)	13 (65)	17 (85)
Spleen	0 (0)	2 (10)	8 (40)	17 (85)	16 (80)	17 (85)
Blood[b]	No	Yes	Yes	Yes	Yes	Yes

[a] This group contained 19 mice. All other groups contained 20 mice.
[b] Bacteremia was determined by pooling samples by group. Only female mice were bacteremic at 24 h postchallenge; both male and female mice were bacteremic at subsequent time points.

TABLE 5 Incidence summary of plague-related microscopic findings

Sample source	Total no. of mice/group[a] by sample collection time (h postchallenge)			
	36	48	60	72
Lung with bronchi				
Infiltrate, mixed-cell/pneumonia[b]	2	8	10	10
Edema, alveolar	1	0	2	5
Bacteria[b]	2	7	9	12
Necrosis[b]	1	2	2	5
Hypertrophy, endothelial	3	7	9	10
Mandibular lymph node				
Infiltrate, neutrophilic	4	8	8	10
Bacteria	2	8	8	9
Necrosis	1	4	7	7
Bronchial lymph node				
Infiltrate, neutrophilic	0	5	7	9
Bacteria	0	4	8	10
Necrosis	0	0	4	6
Spleen				
Infiltrate, neutrophilic	1	11	12	15
Depletion, marginal zone	1	13	2	8
Depletion, white pulp[b]	0	0	10	8
Bacteria (red pulp)	0	2	7	8
Necrosis	0	0	1	4
Liver				
Infiltrate, neutrophilic (sinusoids)	0	8	10	10
Necrosis	0	2	3	9
Bacteria	0	0	3	10

[a] Tissues from 20 mice were evaluated at each sample collection time point. Plague-related microscopic observations were not provided 12 and 24 h postchallenge. One mouse had microscopic evidence of pneumonia at 24 h postchallenge; no additional plague-related microscopic observations were made at this sample collection point.
[b] Histopathological findings also described in human pneumonic plague as reviewed by Adamovicz and Worsham (1).

cytes) adjacent to airways in the lung. This infiltrate was observed at later time points with increased severity. There were no remarkable microscopic lesions present in any other tissues at this time point.

Pneumonia and bacteria were present in 2 mice (10%) at 36 h postchallenge. In 1 of these 2 mice the pneumonia was accompanied by mild alveolar edema and minimal necrosis. Minimal hypertrophy of the endothelial cells lining the vessels of the lung, an early indicator of acute inflammation, was present in two mice. A third mouse with minimal hypertrophy of the endothelial cells had no evidence of an inflammatory cell infiltrate. Neutrophilic infiltrates were present in the mandibular lymph nodes of 4 (20%) mice, 2 of which also contained bacteria.

The spleen of one mouse had moderate depletion of the marginal zone with mild neutrophilic infiltrate. These two findings in the spleen were commonly observed at later time points in the study with increased severity. In general, the inflammatory processes and growth of bacteria were more common in male mice but were slightly more severe in the female mice. Reported observations of bacteria are inclusive of all mice, not just those with pneumonia. No microscopic changes were observed in the liver and bronchial lymph nodes at 36 h postchallenge. A summary of the relevant microscopic findings and micrographs of plague-related lesions are provided in Table 5 and Fig. 3, respectively.

By 48 h postchallenge, multiple microscopic findings in the lung, lymph node, spleen, and liver were observed and considered plague related. Eight mice (40%) had microscopic evidence of pneumonia, with bacteria observed in the lungs of 7 of the 8 mice. Necrosis was present in two of the mice with pneumonia. Minimal hypertrophy of the vascular epithelium of the lung was present in four mice. Three additional mice with minimal hypertrophy of the endothelial cells had no evidence of inflammatory cell infiltrate. Neutrophilic infiltrates were present in the mandibular lymph nodes of 8 (40%) mice and in the bronchial lymph node of 5 (25%) mice. In three mice, both lymph nodes contained neutrophils. Bacteria were observed in 92% of the lymph nodes containing neutrophils. Necrosis was present in the mandibular lymph nodes of four mice. Minimal to moderate depletion of the marginal zone of the spleen was present in 13 (65%) of the mice with a concurrent presence of neutrophils in 11 mice. Bacteria were observed in the red pulp of two mice. Minimal to mild infiltrates of neutrophils in the sinusoids of the liver were present in 8 (40%) mice with necrosis present in 2 (10%) mice. Bacteria were not observed in the liver at this time point.

By 60 h postchallenge, 14 (70%) mice had one or more microscopic finding considered to be plague related. Pneumonia was

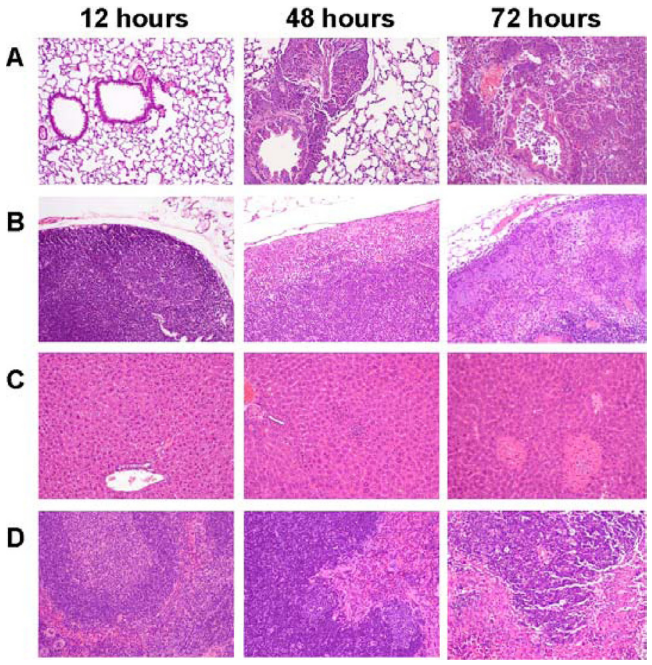

FIG 3 Plague-related lesions in the lung, mandibular lymph node, liver, and spleen at 12, 48, and 72 h following aerosol exposure to *Y. pestis* CO92 (×10 magnification). (A) Lung. Twelve h, normal parenchyma; 48 h, focus of inflammation centered on the airway; 72 h, diffuse infiltrates of neutrophils colocalized with clusters of bacteria. (B) Mandibular lymph node. Twelve h, normal capsular surface with a germinal center (also normal); 48 h, subcapsular sinus filled with neutrophils; 72 h, large clusters of bacteria in both the subcapsular sinus and the parenchyma of the lymph node. (C) Liver. Twelve h, normal parenchyma; 48 h, 3 foci of neutrophilic infiltrates; 72 h, 2 foci of necrosis and 1 focus of neutrophilic infiltrates. (D) Spleen. Twelve h, normal parenchyma; 48 h, increased numbers of neutrophils in the red pulp and a slight decrease in the marginal zone; 72 h, marginal zone is partially depleted and contains bacteria.

observed in the lungs of 10 (50%) mice, with bacteria observed in 9 of the 10 mice. Necrotizing pneumonia and alveolar edema were present in two mice. Minimal to moderate hypertrophy of the vascular epithelium of the lung was present in eight mice. An additional mouse with a mildly hypertrophic vascular epithelium had no evidence of inflammatory cell infiltrate. Seven (35%) mice had neutrophilic infiltrates with coincident bacteria in the bronchial lymph node, whereas bacteria in the absence of neutrophilic infiltrate were observed in one mouse. Necrosis and inflammation were also present in 4 of the 7 mice. Eight (40%) mice had neutrophilic infiltrates and bacteria in the mandibular lymph node; necrosis and inflammation were present in all but one mouse. Minimal to moderate depletion of the marginal zone and white pulp of the spleen was observed in 2 and 10 mice, respectively, with concurrent infiltration of neutrophils in the red pulp. Bacteria were observed in the spleen of 7 mice, with necrosis present in 1 of the mice. Clusters of neutrophils in the sinusoids of the liver were present in 10 (50%) mice with bacteria and necrosis observed in 3 of the 10 mice.

By the final 72-h-postchallenge collection point, multiple microscopic findings in the lung, lymph node, spleen, and liver were observed and considered plague related. Microscopic evidence of pneumonia with bacteria was observed in lung sections of 10 (50%) mice. Inflammation in the lung was necrotizing in 5 of the mice with pneumonia. The hypertrophy of the vascular epithelium was present in 10 mice. Nine mice (45%) had neutrophilic infiltrates in the bronchial lymph node concurrent with bacteria; however, bacteria were present in an additional mouse without an infiltrate of neutrophils. Bacteria were also observed in two mice without microscopic evidence of pneumonia. Neutrophilic infiltrates were observed in the mandibular lymph node of 10 mice (50%), with concurrent bacteria in all but one of the mice. Necrosis was present in 6 bronchial and 7 mandibular lymph nodes. Mild to marked depletion of the marginal zone or white pulp of the spleen was observed in 16 (80%) of the mice, with concurrent infiltrates of neutrophils in the red pulp of all but one mouse. Bacteria were present in the red pulp of half of these mice. Clusters of neutrophils were observed in the liver in 10 mice with associated necrosis, and bacteria were observed in 5 of the mice. Necrosis and bacteria in the absence of a neutrophilic infiltrate were observed in four mice. The liver of one mouse contained bacteria in the absence of additional microscopic observations.

At the last two sample collection points, nine mice exhibited congestion in multiple tissues without the presence of pneumonia. Microscopic observations of bacteria in the lymph nodes, spleen, and liver in the absence of an inflammatory process were present. The marked depletion of the marginal zone in the spleen was also observed.

DISCUSSION

Several small animals have been evaluated as potential models for pneumonic plague (1, 48). Guinea pigs, rabbits, and rats have been used in model development studies; however, each has limitations regarding their suitability as an appropriate animal model for vaccine licensure under the Animal Rule. Guinea pigs are not responsive to F1 and V antigen-based vaccines without the inclusion of oil-based adjuvants which are not licensed for human use (36, 42). In addition, guinea pigs are somewhat resistant to F1 strains of *Y. pestis* that are virulent for other animal species as well as for humans (7, 44). Rabbits have not been established as reliable laboratory models for plague, even though they are susceptible to infection in the wild. Following aerosol challenge, rabbits develop septicemic plague rather than pneumonic plague (33). However, they respond well to vaccination with F1- and V-based vaccines and are often used to make antibodies (20, 28). Although wild rats are associated with natural outbreaks of plague, laboratory strains of rats are more resistant to infection than those of mice or guinea pigs (12).

Several strains of mice have been used to describe the pathogenesis of pneumonic plague (2, 6, 22, 35). Bubeck et al. (6) compared the pathogenesis of pneumonic plague in outbred and inbred strains of mice and found that the kinetics of infection and progression of disease were the same for both strains of mice. We selected the outbred Swiss Webster (CFW) mouse strain for additional characterization in this study as a small-animal model for pneumonic plague based upon proof-of-concept studies demonstrating the immunogenicity and efficacy of the rF1V vaccine (3, 19). Furthermore, the heterogeneous immune responses expected in an outbred strain of mice due to inherent genetic differences may be more reflective of the expected human response than responses expected in an inbred strain of mouse. Lastly, male and female mice were used in this study to evaluate the pathophysiology of disease in both sexes, as recommended in FDA draft guidance (10). Challenge agent, route of exposure, quantification of exposure, and pathogenic determinants, all important characteristics of animal model development that may affect disease, were evaluated in this study. We believe this to be the only published mouse model study specifically designed to fulfill these essential data elements required for animal models as described in FDA draft guidance (10).

Human cases of pneumonic plague are characterized by the presence of lobular pneumonia and consolidation. Lung volume decreases over time as a result of extensive edema and the presence of neutrophils and bacteria. Bacteria are also present in the blood, lymph nodes, and spleen (1). Similar findings were observed in our study, supporting the utility of the Swiss Webster mouse model of pneumonic plague.

Microscopic evidence of pneumonia was observed in a single mouse with a mixed-cell infiltrate 24 h postchallenge. Neutrophils, usually first responders in the immune cell repertoire following bacterial infection (34), were not observed microscopically by 12 or 24 h postchallenge. The delay in the migration of neutrophils to the tissues was likely due to the anti-inflammatory effects of the type three secretion system which allowed the growth of *Y. pestis* in the host (30) by the downregulation of intracellular adhesion molecule-1 (ICAM-1) and E-selectin by *Yersinia* outer protein P (YopP/YopJ) (14). E-selectin expression on endothelial cells assists in neutrophil rolling, and ICAM-1 assists in neutrophil adhesion, arrest, and migration into the tissue. However, by 36 h postchallenge, neutrophilic infiltrates were observed in the lung, mandibular lymph node, and spleen. A concurrent increase in neutrophil counts was also observed in the blood at this time and is consistent with response to infection.

There was a time-dependent increase in the incidence and severity of pneumonia over time. The pneumonia was similar to the exudative pneumonia with edema described for C57BL/6 mice (22) and previously described for Swiss Webster mice (2). Furthermore, mice with pneumonia more commonly had inflammation in the lymph nodes that drain the lung. We also observed a general increase in the incidence and severity of microscopic find-

ings in the lymph nodes, spleen, and liver. The highest incidence of bacteria and neutrophils was in the mandibular lymph node. This may be due to the direct drainage of bacteria from the nasal cavity and pharynx. Bacteria also spread via the blood to colonize tissues, as evidenced by the isolation of bacteria and increased microscopic observations of bacteria in the tissues. Concurrent with the influx of immune cells and bacteria into the lymph nodes was a moderate depletion of the marginal zone of the spleen. The marginal zone is predominantly composed of macrophages, which are important in removing bacteria and viruses and presenting antigens to lymphocytes (11). In general, as these macrophages disappeared from the spleen, the numbers of tissues with bacteria increased, suggesting that the host immune response could no longer control infection.

Scattered neutrophilic infiltrates in the liver were observed by 48 h postchallenge, and the incidence remained relatively steady throughout the remainder of the study. Increases in clinical chemistry values for ALT and AST observed at this time point were consistent with microscopic observations of inflammation and necrosis in the liver. The presence of neutrophils in the liver as well as spleen and lymph nodes at this time was associated with an increase in neutrophil counts in the blood. With this increase in neutrophils in the blood there was a concomitant decrease in circulating lymphocytes 48 h postchallenge. The decrease in lymphocytes may have been secondary to stress, disease, and shock in the mice (38).

By 60 and 72 h postchallenge, mice were observed to have hunched posture and rough fur. The incidence of pneumonia was increased compared to that at previous time points. Inflammation with bacteria in the lymph nodes draining the lung was common in the mice with pneumonia, whereas inflammation and bacteria were observed in the mandibular lymph node of mice without pneumonia. Whether this represents two separate progressions of disease or whether all animals with only mandibular lymph node involvement would have progressed to a pneumonic state is unknown. The depletion of the marginal zone in the spleen and the incidence of neutrophilic infiltrates in the liver also increased. By 72 h postchallenge, large clusters of bacteria had grown in the interstitium around blood vessels, providing strong support for vascular delivery of the bacteria back into the lung. This observation supports the hypothesis (22) that primary pneumonic plague at this stage of disease in mice is a combination of primary and secondary foci of infection.

Our observation that some mice died at these later time points with congestion in multiple tissues or mandibular lymphadenitis without microscopic evidence of pneumonia suggests that the septicemic form of disease can result following exposure via the respiratory route. Indeed, fatal cases of human plague with cervical lymphadenitis have been reported. It has been suggested that these individuals were exposed by the oral and/or aerosol route and developed pharyngeal plague that progressed to a systemic infection rather than the pneumonic form of disease (32, 33). Septic shock induced by hypotension likely was responsible for the deaths in mice with congestion in multiple tissues, and mice with lymphadenitis likely died from Gram-negative sepsis, suggesting disease progression that did not require the development of fulminate pneumonia.

No differences were observed in clinical signs or mortality rate between male and female mice. However, some differences were observed in bacterial burden, hematology parameters, and microscopic evaluations of tissue between male and female mice. While the presence of bacteria in blood was detected 12 h earlier in females than males, the number of tissues with bacteria was slightly higher in male mice. These differences likely are not meaningful given that bacteremia was detected using pooled samples and that the qualitative assessment of bacterial burden in the tissues was performed. Although overall white blood cell counts yielded significant increases in neutrophil counts and a corresponding decrease in lymphocytes at 36 h postchallenge and at subsequent time points, differences in counts between males and females was observed only at the 72-h time point. Female mice exhibited a significantly lower ($P < 0.05$) neutrophil count and a significantly higher ($P < 0.05$) lymphocyte count compared to male mice at this time point, suggesting that the response to an acute inflammatory stimuli was more robust in females. This is supported by microscopic observations of tissue in which the inflammatory processes and growth of bacteria were more common in male mice but were slightly more severe in the female mice. Regardless, these data suggest that both male and female Swiss Webster mice are appropriate models of pneumonic plague.

This study was performed to address the essential data elements needed to establish a relevant animal model, as recommended in FDA draft guidance (10). The data collected from this study using well-characterized challenge material to expose mice in a nose-only aerosol exposure system demonstrate the utility of the Swiss Webster mouse as a model of pneumonic plague that can be used by other researchers investigating plague countermeasures. The characterization of the Swiss Webster mouse model of pneumonic plague in conjunction with the previously developed cynomolgus macaque model (43) concludes animal model development studies currently planned prior to evaluating the efficacy of the rF1V vaccine.

ACKNOWLEDGMENTS

This study was supported by the Chemical-Biological Medical Systems Joint Vaccine Acquisition Program (CMBS/JVAP) contract DAMD 17-98-C8024.

IIT Research Institute (IITRI) is fully accredited by the Association for the Assessment and Accreditation of Laboratory Animal Care International.

We thank Kaylyn Siefkas, Sandra McCurdy, the IITRI technical team, and J. Adam Caulk for excellent technical assistance during this study. We also thank Mary Kate Hart, Shannon Martin, and Jeffrey Shearer for the critical review of the manuscript.

REFERENCES

1. **Adamovicz JJ, Worsham PL.** 2006. Plague, p 107–135. *In* Swearengen JR (ed), Biodefense research methods and animal models. CRC Press, Boca Raton, FL.
2. **Agar SL, et al.** 2008. Characterization of a mouse model of plague after aerosolization of *Yersinia pestis* CO92. Microbiology **154**:1939–1948.
3. **Anderson GW, Heath DG, Bolt CR, Welkos SL, Friedlander AM.** 1998. Short- and long-term efficacy of single-dose subunit vaccines against *Yersinia pestis* in mice. Am. J. Trop. Med. Hyg. **58**:793–799.
4. **Andrews GP, Heath DG, Anderson GW, Welkos SL, Friedlander AM.** 1996. Fraction 1 capsule antigen (f1) purification from *Yersinia pestis* CO92 and from *Escherichia coli* recombinant strain and efficacy against lethal plague challenge. Infect. Immun. **64**:2180–2187.
5. **Barry J.** 1 February 1993. Planning a plague? Newsweek, p 40–41.
6. **Bubeck SS, Cantwell AM, Dube PH.** 2007. Delayed inflammatory response to primary pneumonic plague occurs in both outbred and inbred mice. Infect. Immun. **75**:697–705.
7. **Burrows TW, Bacon GA.** 1958. The effects of loss of different virulence

determinants on the virulence and immunogenicity of strains of *Yersinia pestis*. Br. J. Exp. Pathol. **39**:278.
8. **Cavanaugh DC, Cadigan FC, Williams JE, Marshall JD.** 1982. Plague. *In* Ognibene AJ, Barrett NO (ed), General medicine and infectious disease internal medicine in Vietnam, vol. 2. Office of the Surgeon General and Center of Military History, Washington, DC.
9. **CDC.** 8 November 2011, accession date. Emergency preparedness and response. CDC, Atlanta, GA. http://www.bt.cdc.gov/agent/agentlist-category.asp.
10. **Center for Drug Evaluation and Research.** 2009. Guidance for industry: animal models–essential elements to address efficacy under the Animal Rule. Food and Drug Administration, Department of Health and Human Services, Washington, DC. http://www.fda.gov/downloads/Drugs/GuidanceComplianceRegulatoryInformation/Guidances/UCM078923.pdf.
11. **Cesta MF.** 2006. Normal structure, function and histology of the spleen. Tox. Pathol. **34**:455–465.
12. **Chen TH, Meyer KF.** 1974. Susceptibility and antibody response of *Rattus* species to experimental plague. J. Infect. Dis. **129**(Suppl.):S62.
13. **Chichester JA, et al.** 2009. A single compound two-valent LcrV-F1 vaccine protects non-human primates against pneumonic plague. Vaccine **27**:3471–3474.
13a. **Code of Federal Regulations.** 2002. Title 21. Food and Drugs. Chapter I. Food and Drug Administration. Subpart H. Approval of biological products when human efficacy studies are not ethical or feasible. 21 CFR 601.91.
14. **Cornelis GR.** 2009. Molecular and cell biology aspects of plague. Proc. Natl. Acad. Sci. U. S. A. **97**:8778–8783.
15. **Cornelius CA, et al.** 2008. Immunization with recombinant V10 protects cynomolgus macaques from lethal pneumonic plague. Infect. Immunol. **76**:5588–5597.
16. **Doll JM, et al.** 1994. Cat-transmitted fatal pneumonic plague in a person who traveled from Colorado to Arizona. Am. J. Trop. Med. Hyg. **51**:109–114.
17. **Feodorova VA, Corbel MJ.** 2009. Prospects for new plague vaccines. Expert Rev. Vaccines **8**:1721–1738.
18. **Guyton ACN.** 1947. Measurement of the respiratory volumes of laboratory animals. Am. J. Physiol. **150**:70–77.
19. **Heath DG, et al.** 1998. Protection against experimental bubonic and pneumonic plague by a recombinant capsular F1-V antigen fusion protein vaccine. Vaccine **16**:1131–1137.
20. **Jawetz E, Meyer KF.** 1944. The behavior of virulent and avirulent *P. pestis* in normal and immune experimental animals. J. Infect. Dis. **74**:1.
21. **Johnson D, Vincent J.** 2003. Sampling and sizing of airborne particles. *In* DeNardi SR (ed), The occupational environment: its evaluation, control and management. American Industrial Hygiene Association, Fairfax, VA.
22. **Lathem WW, Crosby SD, Miller VL, Goldman WE.** 2005. Progression of primary pneumonic plague: a mouse model of infection, pathology, and bacterial transcriptional activity. Proc. Natl. Acad. Sci. U. S. A. **102**:17786–17791.
23. **Leary SEC, et al.** 1995. Active immunization with recombinant V antigen from *Yersinia pestis* protects mice against plague. Infect. Immun. **63**:2854–2858.
24. **Marshall JD, Jr, Bartelloni PJ, Cavanaugh DC, Kadull PJ, Meyer KF.** 1974. Plague immunization. II. Relation of adverse clinical reactions to multiple immunizations with killed vaccine. J. Infect. Dis. **129**(Suppl): S19–S25.
25. **Mee C.** 1990. How a mysterious disease laid low Europe's masses. Smithsonian **20**:66–79.
26. **Mett V, et al.** 2007. A plant-produced plague vaccine candidate confers protection to monkeys. Vaccine **25**:3014–3017.
27. **Meyer KF, Cavanaugh DC, Bartelloni PJ, and Marshall JD, Jr.** 1974. Plague immunization. I. Past and present trends. J. Infect. Dis. **129**(Suppl):S13–S18.
28. **Meyer KF.** 1950. Immunity in plague: a critical consideration of some recent studies. J. Immunol. **64**:139.
29. **Morris SR.** 2007. Development of a recombinant vaccine against aerosolized plague. Vaccine **25**:3115–3117.
30. **Nakajima R, Brubaker RR.** 1993. Association between virulence of *Yersinia pestis* and suppressions of gamma interferon and tumor necrosis factor alpha. Infect. Immunol. **61**:23–31.
31. **National Research Council Institute of Laboratory Animal Resources.** 1996. Guide for the Care and Use of Laboratory Animals. National Academies Press, Washington, DC.
32. **Poland JD, Dennis DT.** 1998. Plague, p 545–558. *In* Evans AS, Brachman PS (ed), Infectious diseases of humans: epidemiology and control. Plenum Press, New York, NY.
33. **Pollitzer R.** 1954. Plague. WHO Monogr. Ser. **22**:1.
34. **Rosenberg HF, Gallin JI.** 1999. Inflammation. *In* Paul W (ed), Fundamental immunology. Lippincott-Raven, Philadelphia, PA.
35. **Sha J, et al.** 2008. Braun lipoprotein (Lpp) contributes to virulence of *Yersiniae*: potential role of Lpp in inducing bubonic and pneumonic plague. Infect. Immun. **76**:1380–1409.
36. **Spivack ML, et al.** 1958. The immune response of the guinea pigs to the antigens of *Pasteurella pestis*. J. Immunol. **80**:132–141.
37. **Stenseth NC, et al.** 2008. Plague: past, present and future. PLoS Med. **5**:9–13.
38. **Stockham SL, Scott MA.** 2002. Leukocytes. *In* **Fundamentals of veterinary clinical pathology. Iowa State Press, Ames, IA.**
39. **Straley SC, Skrzpek E, Plano GV, Bliska JB.** 1993. Yops of *Yersinia* spp. pathogenic for humans. Infect. Immun. **61**:3105–3110.
40. **United States Army Medical Research Institute of Infectious Diseases.** 2005. Medical management of biological casualties handbook, 6th ed. United States Army Medical Research Institute of Infectious Diseases, Frederick, MD.
41. **University of Minnesota.** 8 November 2011, accession date. Reference values for laboratory animals. University of Minnesota, St. Paul, MN. http://www.ahc.umn.edu/rar/refvalues.html.
42. **von Metz E, Eisler DM, Hottle GA.** 1971. Immunogenicity of plague vaccines in mice and guinea pigs. Appl. Microbiol. **22**:84.
43. **Warren R, et al.** 2011. Cynomolgus macaque model for pneumonic plague. Microb. Pathog. **50**:12–22.
44. **Welkos Davis SLKM, Pitt LM, Worsham PL, Friedlander AM.** 1995. Studies on the contribution of the F1 capsule-associated plasmid pFra to the virulence of *Yersinia pestis*. Contrib. Microbiol. Immunol. **13**:299–305.
45. **Williams P, Wallace D.** 1989. Unit 731: Japan's secret biological warfare in World War II. The Free Press, New York, NY.
46. **Williams RC, Gewurz H, Quie PG.** 1972. Effects of faction I from *Yersinia pestis* on phagocytosis *in vitro*. J. Infect. Dis. **126**:235–241.
47. **Williamson ED, et al.** 2011. Recombinant (F1+V) vaccine protects cynomolgus macaques against pneumonic plague. Vaccine **29**:4771–4777.
48. **Williamson ED.** 2009. Plague. Vaccine **27**:D56–D60.
49. **Williamson ED, et al.** 1995. A new improved sub-unit vaccine for plague: the basis of protection. FEMS Immun. Med. Micro. **12**:223–230.
50. **World Health Organization.** 8 November 2011, accession date. WHO, Geneva, Switzerland. www.who.int/mediacentre/factsheets/fs267/en/.